

A novel dumbbell-shaped coil featured with cross coupling suppression for long distance relay wireless power transfer applications

Xiaoxiong Zhang, Bin Luo^{a)}, Yao Hu, Shengbin Liu,
and Chenming Zhong

School of Information Engineering, Nanchang University,

Xuefu Avenue 999, Honggutan New District, Nanchang 330031, Jiangxi, China

a) luobin@ustc.edu

Abstract: The use of multi-resonators for medium-range wireless power transfer (WPT) systems is an important concern; the cross-couplings between non-adjacent coils have an adversely impact on the transmission distance and efficiency of the system. This paper proposes a dumbbell-shaped (DS) coil in a WPT system. The DS coil structure was analyzed theoretically and verified experimentally. The proposed scheme eliminates cross-couplings between non-adjacent coils in the multiple resonator system to resolve frequency drift, and improve the transmission distance and efficiency in the multiple resonator system. The scheme features a coplanar structure which can secure direct-coupling and save space when applied in the home, office, and public areas.

Keywords: cross-coupling, long distance, relay resonator, wireless power transfer (WPT)

Classification: Microwave and millimeter-wave devices, circuits, and modules

References

- [1] M. Catrysse, *et al.*: “An inductive power system with integrated bi-directional data-transmission,” *Sens. Actuators A Phys.* **115** (2004) 221 (DOI: [10.1016/j.sna.2004.02.016](https://doi.org/10.1016/j.sna.2004.02.016)).
- [2] J. Sallan, *et al.*: “Optimal design of ICPT systems applied to electric vehicle battery charge,” *IEEE Trans. Ind. Electron.* **56** (2009) 2140 (DOI: [10.1109/TIE.2009.2015359](https://doi.org/10.1109/TIE.2009.2015359)).
- [3] H. Cao, *et al.*: “An implantable, batteryless, and wireless capsule with integrated impedance and pH sensors for gastroesophageal reflux monitoring,” *IEEE Trans. Biomed. Eng.* **59** (2012) 3131 (DOI: [10.1109/TBME.2012.2214773](https://doi.org/10.1109/TBME.2012.2214773)).
- [4] A. Abdolkhani, *et al.*: “Wireless charging pad based on travelling magnetic field for portable consumer electronics,” *IECON 2013-39th Annual Conference of the IEEE Industrial Electronics Society* (2013) 1416 (DOI: [10.1109/IECON.2013.6699340](https://doi.org/10.1109/IECON.2013.6699340)).

- [5] A. Kurs, *et al.*: “Wireless power transfer via strongly coupled magnetic resonances,” *Science* **317** (2007) 83 (DOI: [10.1126/science.1143254](https://doi.org/10.1126/science.1143254)).
- [6] J. Park, *et al.*: “Investigation of adaptive matching methods for near-field wireless power transfer,” *IEEE Trans. Antennas Propag.* **59** (2011) 1769 (DOI: [10.1109/TAP.2011.2123061](https://doi.org/10.1109/TAP.2011.2123061)).
- [7] B.-C. Park and J.-H. Lee: “Adaptive impedance matching of wireless power transmission using multi-loop feed with single operating frequency,” *IEEE Trans. Antennas Propag.* **62** (2014) 2851 (DOI: [10.1109/TAP.2014.2307340](https://doi.org/10.1109/TAP.2014.2307340)).
- [8] E. Waffenschmidt and T. Staring: “Limitation of inductive power transfer for consumer applications,” 13th European Conference on Power Electronics and Applications, EPE’09 (2009) 1.
- [9] J. O. Mur-Miranda, *et al.*: “Wireless power transfer using weakly coupled magnetostatic resonators,” 2010 IEEE Energy Conversion Congress and Exposition (ECCE) (2010) 4179 (DOI: [10.1109/ECCE.2010.5617728](https://doi.org/10.1109/ECCE.2010.5617728)).
- [10] C. Park, *et al.*: “Innovative 5-m-off-distance inductive power transfer systems with optimally shaped dipole coils,” *IEEE Trans. Power Electron.* **30** (2015) 817 (DOI: [10.1109/TPEL.2014.2310232](https://doi.org/10.1109/TPEL.2014.2310232)).
- [11] J. Acero, *et al.*: “Analysis and modeling of planar concentric windings forming adaptable-diameter burners for induction heating appliances,” *IEEE Trans. Power Electron.* **26** (2011) 1546 (DOI: [10.1109/TPEL.2010.2085453](https://doi.org/10.1109/TPEL.2010.2085453)).
- [12] R. R. A. Syms, *et al.*: “A theory of metamaterials based on periodically loaded transmission lines: Interaction between magnetoinductive and electromagnetic waves,” *J. Appl. Phys.* **97** (2005) 064909 (DOI: [10.1063/1.1850182](https://doi.org/10.1063/1.1850182)).
- [13] J. Kim, *et al.*: “Efficiency analysis of magnetic resonance wireless power transfer with intermediate resonant coil,” *IEEE Antennas Wireless Propag. Lett.* **10** (2011) 389 (DOI: [10.1109/LAWP.2011.2150192](https://doi.org/10.1109/LAWP.2011.2150192)).
- [14] M. Kiani, *et al.*: “Design and optimization of a 3-coil inductive link for efficient wireless power transmission,” *IEEE Trans. Biomed. Circuits Syst.* **5** (2011) 579 (DOI: [10.1109/TBCAS.2011.2158431](https://doi.org/10.1109/TBCAS.2011.2158431)).
- [15] W. Zhong, *et al.*: “General analysis on the use of Tesla’s resonators in domino forms for wireless power transfer,” *IEEE Trans. Indust. Electron.* **60** (2013) 261 (DOI: [10.1109/TIE.2011.2171176](https://doi.org/10.1109/TIE.2011.2171176)).
- [16] E. Shamonina, *et al.*: “Magneto-inductive waveguide,” *Electron. Lett.* **38** (2002) 371 (DOI: [10.1049/el:20020258](https://doi.org/10.1049/el:20020258)).
- [17] C. K. Lee, *et al.*: “Effects of magnetic coupling of nonadjacent resonators on wireless power domino-resonator systems,” *IEEE Trans. Power Electron.* **27** (2012) 1905 (DOI: [10.1109/TPEL.2011.2169460](https://doi.org/10.1109/TPEL.2011.2169460)).
- [18] A. P. Sample, *et al.*: “Analysis, experimental results, and range adaptation of magnetically coupled resonators for wireless power transfer,” *IEEE Trans. Ind. Electron.* **58** (2011) 544 (DOI: [10.1109/TIE.2010.2046002](https://doi.org/10.1109/TIE.2010.2046002)).
- [19] M. Q. Nguyen, *et al.*: “Multiple-inputs and multiple-outputs wireless power combining and delivering systems,” *IEEE Trans. Power Electron.* **30** (2015) 6254 (DOI: [10.1109/TPEL.2015.2438016](https://doi.org/10.1109/TPEL.2015.2438016)).
- [20] T. Imura: “Equivalent circuit for repeater antenna for wireless power transfer via magnetic resonant coupling considering signed coupling,” 2011 6th IEEE Conference on Industrial Electronics and Applications (ICIEA) (2011) 1501 (DOI: [10.1109/ICIEA.2011.5975828](https://doi.org/10.1109/ICIEA.2011.5975828)).
- [21] M. Q. Nguyen, *et al.*: “A study of coil orientations to enhance the transfer efficiency of a multi-repeater wireless power transmission system,” 2014 Asia-Pacific Microwave Conference (APMC) (2014) 1354.
- [22] M. Q. Nguyen, *et al.*: “Wireless power transfer via air and building materials using multiple repeaters,” 2014 Texas Symposium on Wireless and Microwave Circuits and Systems (WMCs) (2014) 1 (DOI: [10.1109/WMCs.2014.7015877](https://doi.org/10.1109/WMCs.2014.7015877)).

- [23] S. Raju, *et al.*: “Modeling of mutual coupling between planar inductors in wireless power applications,” IEEE. Trans. Power Electron. **29** (2014) 481 (DOI: [10.1109/TPEL.2013.2253334](https://doi.org/10.1109/TPEL.2013.2253334)).
- [24] S. I. Babic and C. Akyel: “Calculating mutual inductance between circular coils with inclined axes in air,” IEEE Trans. Magn. **44** (2008) 1743 (DOI: [10.1109/TMAG.2008.920251](https://doi.org/10.1109/TMAG.2008.920251)).
- [25] F. Y. Watanabe: “Compensation of cross-coupling stiffness and increase of direct damping in multirecess journal bearings using active hybrid lubrication,” Part I-Theory J. (2004) (DOI: [10.1115/1.1631015](https://doi.org/10.1115/1.1631015)).
- [26] A. Kurs, *et al.*: “Wireless power transfer via strongly coupled magnetic resonances,” Science **317** (2007) 83 (DOI: [10.1126/science.1143254](https://doi.org/10.1126/science.1143254)).
- [27] X. Wei, *et al.*: “A critical review of wireless power transfer via strongly coupled magnetic resonances,” Energies **7** (2014) 4316 (DOI: [10.3390/en7074316](https://doi.org/10.3390/en7074316)).
- [28] Z. Yalong, *et al.*: “Design of wireless power supply system for the portable mobile device,” 2013 IEEE International Wireless Symposium (IWS) (2013) 1 (DOI: [10.1109/IEEE-IWS.2013.6616717](https://doi.org/10.1109/IEEE-IWS.2013.6616717)).

1 Introduction

In recent years, the inductive coupling wireless power transfer (WPT) systems have become ubiquitous throughout our daily lives [1]. The inductive coupling technique can be very efficient when the primary and secondary coils are in close proximity to each other. The efficiency of any inductive coupled system is markedly affected by the axial and angular misalignment between coils. The magnetic coupling resonant coupling (MCR) WPT systems work based on the principle that resonators are tuned at the same resonant frequency, which allows them to effectively and efficiently exchange energy from at a long operating distance compared to inductive coupling systems [2]. The technology has been used in low-power applications such as electric toothbrushes and portable electronic devices [3, 4]. The transmission distance and efficiency of the MCR-WPT systems are common research subjects. Single-source and single-load systems with impedance matching and frequency tracking have been researched extensively in regards to improve transmission efficiency in the mid-range MCR-WPT systems [5, 6]. In [7], defined the mid-range the MCR-WPT systems of wireless power transfer as transmission distance r any greater than three times the diameter d of the primary or secondary; that is, $d/r > 3$, and the transmission efficiency decays exponentially as the transfer distance increases. The transmission distance of the single-source and single-load system is still a critical constraint upon wireless power transfer [8, 9]. Recent efforts to increase the size of the coil and operating frequency of the system have been successful in extending the transfer distance [10]. Once the system operating frequency reaches over-mega-hertz, however, the winding loss grows excessive [11], and the coil takes up an unwanted amount of space. Further, when the system works in the sub-mega-hertz for mid-range WPT, coils fabricated from metamaterial are very expensive [12]. In an effort to resolve transmission distance and efficiency issues, the effects of relay coil was first proposed by Kim et al. [13]. As the distance of the receiving coil from the transmitting coil increases, the relay coil can more effectively enhance the transmission efficiency of the system [14]. A

Domino-Resonator System working in the operating frequency of 500 kHz can increase the transmission distance [15]. The path can be flexibly adjusted by rearranging the relay coils [16, 17]. These studies overlooked the effects of cross-coupling, which introduces frequency drift into the system. In the multi-relay WPT system, the cross-coupling between non-adjacent coils (an interval of one coil) must be accounted for properly while the others can be ignored [18]. In the multiple-inputs and multiple-outputs system, changing the position of the relay coil can reduce cross-coupling, but the limited position of relay is not convenient in practical applications [19]. Relay coils must occupy a great deal of space to eliminate cross-coupling [20, 21].

We propose an overlapped Dumbbell-Shaped (DS) magnetic resonant coupling wireless power transfer system (DS-WPT) which combines domino and array structures (Fig. 1) as a response to the cross-coupling caused the problems in the multiple resonator system. The cross-coupling between non-adjacent coils adversely impacts the system’s frequency drift, transmission distance and efficiency; the DS (coplanar) structure resolves the oversize problem inherent to the domino structure while obtaining better direct-coupling. In the actual environment, when the medium between the coils is a wall or ceiling (i.e., wood, Plexiglas, or other non-metallic material,) there is almost no impact on the WPT system [22]. The DS-WPT system can be applied in the home, office, and public areas easily as it is compact in size and can be hidden in the wall, floor, or furniture, and the system can be designed as a track or charging road to service electric vehicles and factory robots.

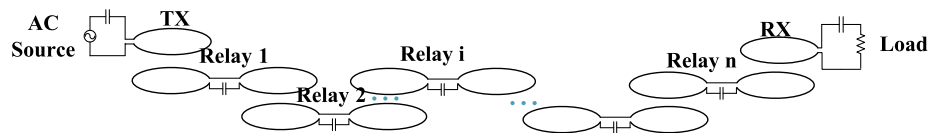


Fig. 1. DS-WPT system, where TX and RX are coplanar.

2 Dumbbell-shaped WPT system model

2.1 Analysis of dumbbell-shaped coil

The primary focus of this study was coil structure. We propose a DS coil structure to manage cross-coupling problems impacting the multi-resonator system between non-contiguous resonators. The DS is mainly composed of L_a and L_b circular coils, which are fabricated from the same material; L_a and L_b , are connected positively and reversely, as shown Fig. 2. The positively connected DS coil can be expressed by the following series inductance equation (1):

$$L = L_a + L_b - 2M_{ab} \quad (1)$$

The reversely connected DS coil can be expressed as follows (2):

$$L = L_a + L_b + 2M_{ab} \quad (2)$$

Where mutual inductance M_{ab} can be calculated via Neumann equation [23, 24]. The M_{ab} value is affected by the shape, size, and relative position of the coil and the surrounding magnetic medium; it is in inverse proportion to the relative distance

d_{ab} between the coil of L_a and L_b . Consequently, when d_{ab} increases to the appropriate value, the M_{ab} approaches to zero.

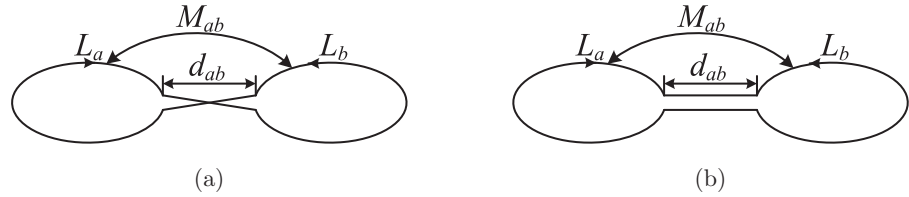


Fig. 2. The DS Coils: (a) “DS connected reversely”; (b) “DS connected positively”.

In the multi-resonator system, large direct-coupling (DC) and small cross-coupling (CC) are deployed to increase transmission efficiency and transmission power. The domino WPT system relay coil structure is in vertical arrangement [15]. Three-coil structure is used in the vertical arrangement and DS connected reversely and positively arrangement three-coil structure, when the single-turn coil radius $r = 1$ m, the resulting changes in the mutual inductance of DC, CC and the distance of coil centers can be obtained as shown in Fig. 3. However, the DC of DS structure coil connected reversely and positively is much larger than that of the traditional domino structure, and the dc of DS structure coil connected positively is slightly greater than the DC of the DS structure coil connected reversely. The DS structure coil connected reversely and positively coil’s CC is rapidly decreasing and approaches zero when the distance of the coil center increases.

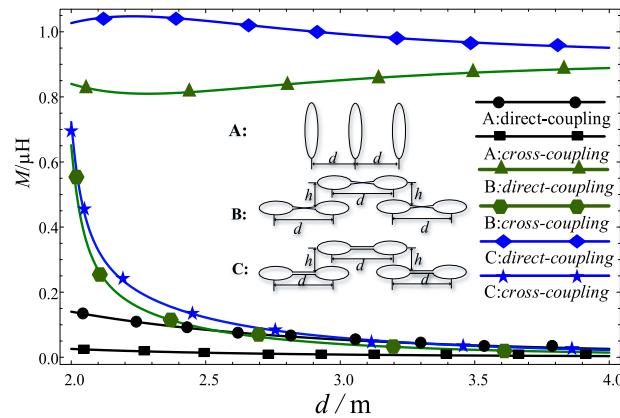


Fig. 3. The CC and DC curves of traditional domino structure coil, and DS structure coil connected reversely and positively, where single-turn coil radius $r = 1$ m, h is set as 0.6 m.

The three-coil CC/DC changed as the distance of the coil centers changed as shown in Fig. 4. The CC/DC of the DS connected reversely and positively structure is much larger than that of the traditional domino structure as distance increased to 2.3 m, and CC/DC of the DS coil connected positively structure is slightly greater than the DS coil connected reversely structure.

The DS coil outperforms the traditional domino structure coil, and the DS coil connected positively structure slightly outperforms the DS coil connected reversely

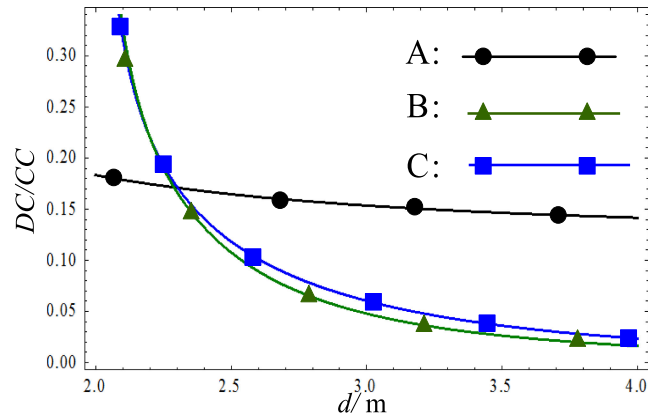


Fig. 4. DC/CC curves: (A) traditional domino structure coil, (B) DS structure coil connected reversely and (C) DS structure coil connected reversely positively.

structure. The DS coil connected positively coil has higher direct-coupling and less cross-coupling, and the distance of centers has little effect on the dc and cc of the DS coil as distance increased to the appropriate value. To this effect, employing a DS coil positively relay coil structure to form a general domino MCR-WPT system can eliminate cross-coupling between non-adjacent coils and weaken the impact of coil distance on the system.

2.2 Parametric analysis of traditional domino WPT system

The CC affected the performance of the system [25], as shown in Fig. 2, the system based on DS composite coils, was designed with bus-type topology. The structure is simple, flexible, reliable, and can be conveniently expanded with a transmitting coil (TX) and receiving coil (RX) as the end device. To save space, the DS relay coil (Relay n) is designed as a ladder and coplanar type structure. It can be easily placed in the floor or walls for practical application.

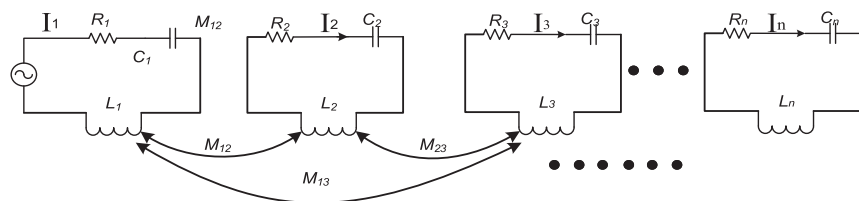


Fig. 5. Circuit model of an n-resonator WPT system.

Circuit theory is commonly used to model domino-resonator WPT systems [26]. The n-resonator circuit model is shown in Fig. 5. According to Kirchhoff's law, the circuit equation of this system is as follows [27]:

$$ZI = U \quad (3)$$

The impedance matrix Z is as follows:

$$\begin{bmatrix} R_1 + j\left(\omega L_1 - \frac{1}{\omega C_1}\right) & j\omega M_{12} & \cdots & j\omega M_{1n} \\ j\omega M_{21} & R_1 + j\left(\omega L_2 - \frac{1}{\omega C_2}\right) & \cdots & j\omega M_{2n} \\ \vdots & \vdots & \ddots & \vdots \\ j\omega M_{n1} & j\omega M_{n2} & \cdots & R_L + R_n + j\left(\omega L_n - \frac{1}{\omega C_n}\right) \end{bmatrix} \quad (4)$$

where R_1 is the internal resistance of the AC power supply plus the loss resistance of the circuit, R_n is the loss resistance of each circuit loop (including storage capacitors and storage resistors), R_L is the load resistance, L_n is the coil inductance, C_n is the tuning capacitor, M_{ab} is the mutual inductance, and ω is the operating angular frequency. All the resonators are tuned at the resonant frequency ω , i.e.

$$\omega = \frac{1}{\sqrt{L_1 C_2}} = \dots = \frac{1}{\sqrt{L_n C_n}} \quad (5)$$

The current equation of the load loop can be determined by solving Eq. (5), and thus the efficiency of the wireless power transmission can be expressed as:

$$\eta = \frac{I_n^2 R_L}{I_1^2 R_1 + I_2^2 R_2 + \dots + I_n^2 (R_n + R_L)} \quad (6)$$

2.3 Comparative analysis of the general domino WPT system and DS-WPT system

The CC in the WPT system causes frequency drift [28]. The DS coil is a better solution to restrain the CC between non-adjacent coils. We ran a comparative analysis to elucidate the effects of CC on the domino MCR-WPT system and the DS MCR-WPT system Fig. 6.

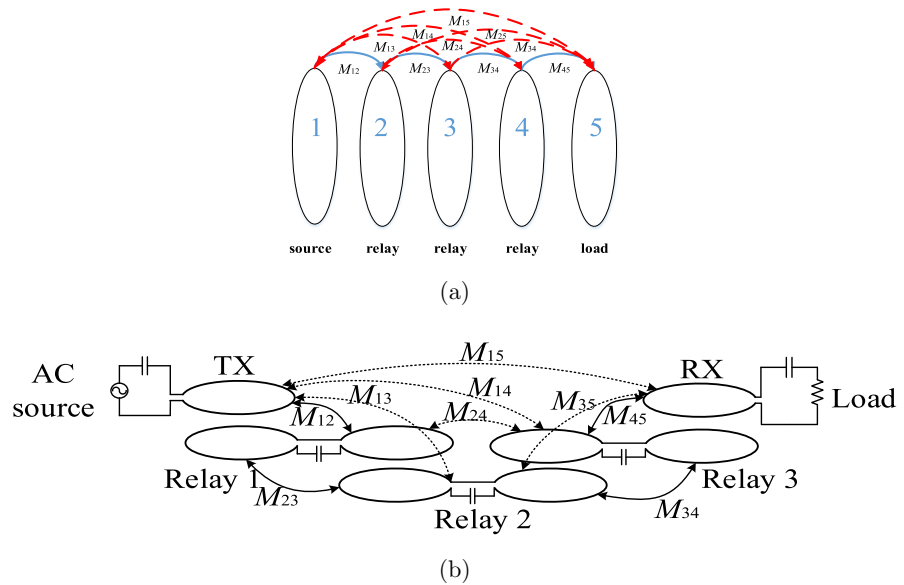


Fig. 6. (a) “The five-resonator domino MCR-WPT system”; (b) “Five-resonator DS MCR-WPT System”.

The coils are equally spaced to obtain the maximum possible transmission efficiency [11], so, the DC are equal to that $M_{12} = M_{23} = M_{34} = M_{45} = 13.6 \mu\text{H}$, in

the domino MCR-WPT system and the DS MCR-WPT system. There are both CC and DC in the domino MCR-WPT system. The CC are as follow $M_{13} = M_{24} = M_{35} = 3 \mu\text{H}$, $M_{14} = M_{25} = 1 \mu\text{H}$, $M_{15} = 0.6 \mu\text{H}$. According to the 2.2 section the DC is much greater than the CC in the DS MCR-WPT system. So the CC can be ignored. The parameters of the LC resonators in the two systems are the same, as shown in Table I.

Table I. Parameters of the LC resonators in the two systems

Inductance (μH)	101.7
Capacitance (nF)	30.78
Loss resistance (Ω)	0.4
Resonance frequency (kHz)	90

When the AC source is 5 V and load resistance is 20Ω , the transmission efficiency can be obtained by (6). In the domino MCR-WPT system, the amplitude curve of the load voltage $|V_L|$ and transmission efficiency of the system at different operating frequencies are calculated by Wolfram Mathematica software, as shown in Fig. 7. When the operating frequency was 90 kHz (resonant frequency) the efficiency of the system was 70.8% and $|V_L|$ was 5.119 V in the top right of the valley. When the operating frequency was 91 kHz, the efficiency reached a peak at 71.6%, while $|V_L|$ was 4.655 V at its peak and fluctuated smoothly. Thus, in the case of the CC between adjacent coils in the domino MCR-WPT system, the optimum frequency of the system would drift significantly. In the DS MCR-WPT system, when the operating frequency $f = 90 \text{ kHz}$, the transmission efficiency was 73.2% which is greater than the maximum transmission in the system with CC. The load voltage $|V_L|$ was 4.68 V in the valley. At resonant frequency $f = 90 \text{ kHz}$, the frequency of the system does not drift and system performance is optimal.

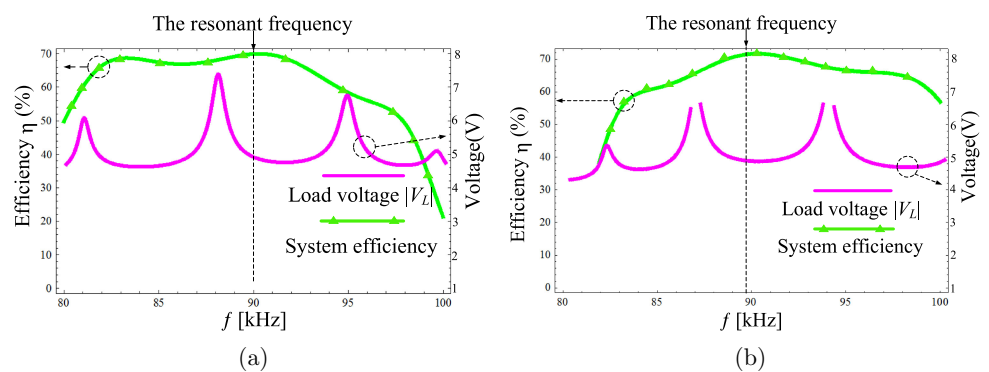


Fig. 7. The calculated values of the load voltage $|V_L|$ and the system efficiency: (a) “The domino MCR-WPT system”; (b) “The DS MCR-WPT system”.

The spatial arrangement of DS MCR-WPT system is flat, and the space of domino MCR-WPT system structure is vertical. When the mutual inductance between the adjacent coils of the two systems is $13.6 \mu\text{H}$, the transmission distance of the domino MCR-WPT system is 40 cm, and the distance of the DS MCR-WPT

system is 150 cm. Therefore, the transmission distance of DS MCR-WPT is much larger than the domino MCR-WPT system. On the basis of the same data from two systems, transmission efficiency of different transmission distance can be obtained, as shown in Fig. 8. It is found that the transmission distance has a great effect on the transmission efficiency of the domino MCR-WPT system [15], but, the transmission distance of the DS MCR-WPT has no effect on the transmission efficiency. The DS MCR-WPT system is a better solution to the problem which the CC between non-adjacent coils caused by frequency drift, efficiency the system.

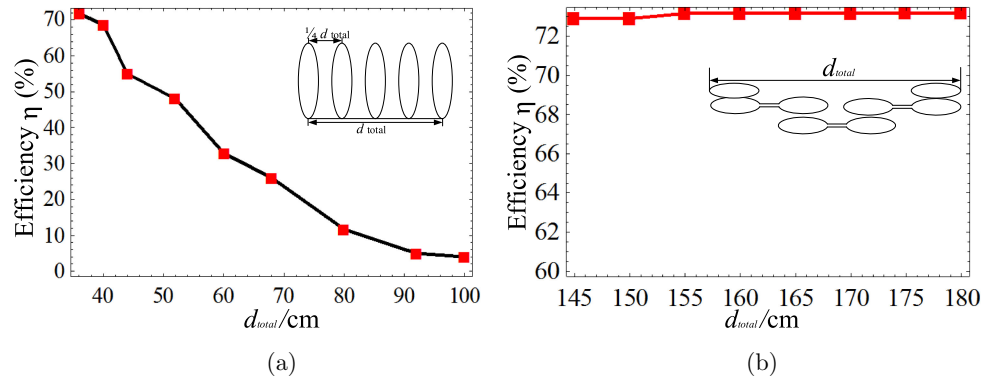


Fig. 8. Measured transmission efficiencies of the equal-spacing domino WPT system and DS MCR-WPT system: (a) “The domino MCR-WPT system”; (b) “The DS MCR-WPT system”.

3 Experimental validation of DS MCR-WPT system

This experimental platform was comprised of a single-source, three-relay single-load MCR-WPT system tasked with lighting an LED (Fig. 9(b)). The AC source in our setup was a half-bridge inverter composed of TL494 chips, IR2110 chips, and IRF540 mos, the output impedance is zero, to this effect, the vector network analyzer (VNA) did not apply in this experiment. The source output voltage was a square wave as-measured with an oscilloscope for no-load, as shown in Fig. 9(b);

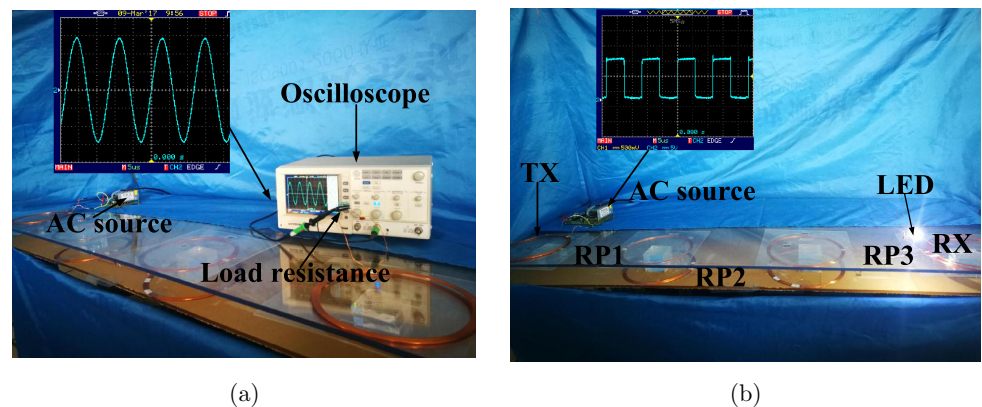


Fig. 9. Dumbbell-Shaped domino MCR-WPT system experiment platform: (a) “Experiment platform rendering to light a LED, the square wave is measured with an oscilloscope for no-load”; (b) “Experiment platform rendering with a 20 Ω resistive load”.

the peak-to-peak value (V_{pp}) was 14 V, the duty cycle was 50.43%, and the operating frequency was 85.75 kHz. The AC source was connected to the TX, which delivered power to the DS RP (DS-RP). For maximum power transmission, the TX and DS-RP were in a coaxial arrangement with center distance of 1.2 cm. Three DS-RP coils were placed in ladder-shaped formation and the first DS relay's rear-end coil was coaxial to the second DS relay's front coil with a center distance of 2 cm; the back end of the system was placed in the same arrangement to obtain maximum transmission efficiency. The end of the DS-RP delivered power in series with the LED. The experimental platform successfully lit the LED via the DS MCR-WPT system. The TX and the RX were coplanar. This structure, as mentioned above, can be conveniently built into walls, floors, or furniture to save space.

The mutual inductance between the TX, the RX and the DS-RP is $13.5 \mu\text{H}$, between the DS-RP coils is $10.5 \mu\text{H}$. The others parameters as shown in Table II. When the load resistance was 20Ω and the transmission distance was 1.5 m, the experimental platform performed as shown in Fig. 9(a). The output and input voltage values are measured using an oscilloscope, and the output and input power values can be obtained, so the system transmission efficiency can be obtained [15]. The measured value load voltage V_L and the system transmission efficiency along the frequency curve was determined per the oscilloscope range from 82.0 kHz and 90.0 kHz and compared to the calculated values, as shown in Fig. 10(a) and Fig. 10(b). In the frequency range from 85.0 kHz to 86.5 kHz, the measured value

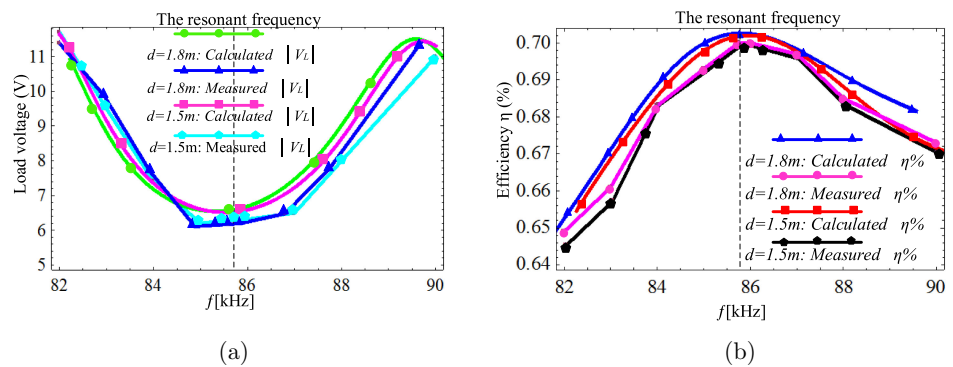


Fig. 10. (a) “Measured value of the voltage magnitude compared with calculated value for the transmission distance is 1.5 m and 1.8 m”; (b) “Measured value of the system efficiency compared with calculated value for the transmission distance is 1.5 m and 1.8 m”.

Table II. Experiment parameters

Coil	TX	RP	RX
Radius (cm)	10	10	10
Inductance (μH)	46.31	93.85	46.31
Turns number	10	10	10
Compensation capacitor (nF)	71	37	71
Loss resistance (Ω)	0.4	0.9	0.4
Wire diameter (mm)	1	1	1

and calculated value error were smaller than those in other ranges. The transmission efficiency reached the maximum at resonant frequency of 85.75 kHz. In the frequency range from 85.0 kHz to 86.5 kHz, the measured and calculated values were closer than those in other ranges (similar to the voltage $|V_L|$ curve). The optimum operation frequency of the system did not drift.

We ran a comparative analysis to elucidate the effects of transmission distance on DS MCR-WPT system. The voltage V_L and the transmission efficiency along the frequency curve at the transmission distance $d = 1.5$ m and $d = 1.8$ m, compared to the calculated values as shown in the Fig. 10(a) and Fig. 10(b). The measured value and calculated value error were smaller, and the voltage V_L and the transmission efficiency change are very small. Therefore, the transmission distance has little effect on the system. Based on the above, one can draw a conclusion that the DS MCR-WPT can be extended transmission distance per the needs of the application environment.

4 Conclusion

In this paper, the proposed DS coil structure was analyzed theoretically and verified experimentally. The DS connected positively coil has higher DC and less CC, it can be to eliminate CC between non-adjacent coils. The structure was applied to a DS MCR-WPT system and compared against a traditional domino WPT system. Simulation and experimental results show that the DS MCR-WPT can significantly improve the transmission distance and efficiency of the system, and the impedance matrix of the DS MCR-WPT system was easier to analyze. At the resonant frequency, the efficiency of the system reached its maximum and the frequency of the system did not drift.

The transmission distance has little effect on the system. The DS MCR-WPT system can extend transmission distance. Moreover, since the DS MCR-WPT is a coplanar structure; it can be applied in home, office, or public areas conveniently by building it into walls, floors, or furniture to save space. The DS MCR-WPT system could also be designed as a track or charging road to service electric vehicles and factory robots.

Acknowledgments

This work was supported by the National Natural Science Foundation of China under grant number 61461031, Natural Science Foundation of Jiangxi, China under grant number 20161BAB202044 and Graduate Student Innovation Special Funds of Nanchang University, China under grant number CX2016273.